Journal of Petroleum Science and Engineering ∎ (∎∎∎∎) ∎∎∎–∎∎∎

Contents lists available at ScienceDirect

Journal of Petroleum Science and Engineering

journal homepage: www.elsevier.com/locate/petrol

Improved Correlations for Heavy-Oil Viscosity Prediction with NMR

Magdalena Sandor*, Yuesheng Cheng, Songhua Chen

Halliburton, 3000 North Sam Houston Pwky E, Houston, TX 77032, USA

ARTICLE INFO

Article history:
Received 21 May 2016
Received in revised form
17 August 2016
Accepted 3 September 2016

Keywords:
Nuclear magnetic resonance
Heavy oil
Viscosity
T2 relaxation
T1 relaxation
Hydrogen index (HI)

ABSTRACT

Delineation of the viscosity in heavy-oil reservoirs is viable for heavy-oil exploration and production activities. Low-field nuclear magnetic resonance (NMR) relaxometry has proven to be a powerful tool for a downhole assessment of heavy-oil viscosity. This prediction is derived from the sensitive relationship between viscosity- and NMR-measured properties, such as spin-spin (T_2) and spin-lattice (T_1) relaxation. In this paper, we demonstrate the versatility of NMR relaxometry by presenting three different approaches for obtaining viscosity correlations that incorporate T_1, T_2, and hydrogen-index (HI) data as a function of temperature and five inter-echo spacings (TE) to account for the signal loss of fast-relaxing components in heavy oil. The results of this work show that NMR-relaxometry measurements correlate very well with heavy-oil viscosities and that each methodology demonstrates reasonable success with heavy-oil predictions. In addition, these relationships demonstrate substantial correlation improvement, especially in comparison with other published relationships that are also tested. Lastly, insight regarding heavy-oil-sample storage time and emulsion is briefly discussed to emphasize the significance of fluid-sample handling within the scheme of heavy-oil viscosity prediction and core/fluid-analysis protocols. Viscosities predicted with a correlation derived from aged and emulsified samples were observed to be within a 17% error in comparison with those predicted with a correlation developed from recently collected heavy oils. From a well-logging point of view, the uncertainty introduced by using aged samples for the interpretation of well-logging data is not considered excessive and may be correctable. These results give new and valuable insight into the considerations that are necessary for sufficient core and fluid analysis.

1. Introduction

Accurate predictions of fluid viscosities are essential to the economic evaluation and production strategies of hydrocarbon-bearing reservoirs. Low-field NMR studies of fluids have demonstrated significant potential as sensitive tools that could be used to predict heavy-oil viscosity through measurements of spin-lattice and spin-spin relaxation times (Kleinberg and Vinegar, 1996; Bryan et al., 2005; LaTorraca et al., 1999; Zhang et al., 1998; Cheng et al., 2009; Ahmed et al., 2014; Zega et al., 1990). Viscosity is one of the most important physical properties of heavy oil that governs the assessment of recoverable reserve estimates and well completion. For light oils, the relationship between NMR relaxation time and viscosity is well understood as $T_1 = T_2 \sim 1/\eta$ and is based on the Stokes-Einstein relationship of viscosity and rotational diffusion. Some of the challenges associated with heavy oil come from the wide range of chemical compounds, ranging from small to complex large molecular weight components (such as wax and asphaltene molecules) (Gawrys et al., 2006; Visintin et al., 2005). The molecular motions of these hydrocarbon components are not fast enough to average out the dipole-dipole interactions of neighboring spins. As a result, T_1 and T_2 distributions of heavy oils are very broad to reflect the molecular sizes of all the constituents within the fluid.

The application and development of NMR relaxometry to viscous oils has gained widespread popularity owing to its potential and promise as a reliable technique for viscosity predictions. Previous NMR viscosity models have incorporated parameters, such as hydrogen index, concepts related to non-Arrhenius dynamics, petroleum viscosity constraints, and instrument and logging-tool parameters (Kleinberg and Vinegar, 1996; Bryan et al., 2005; LaTorraca et al., 1999; Zhang et al., 1998; Cheng et al., 2009; Ahmed et al., 2014; Zega et al., 1990). However, many challenges still exist for the development of robust heavy-oil NMR viscosity-prediction models. In practice, it is often observed that NMR viscosity models derived for heavy oils from a particular field do not necessarily work when applied to other heavy oils, resulting in the over or underestimation of viscosities by as much as over a factor of 3 (Cheng et al., 2009; Ahmed et al., 2014, 2012). Some of these discrepancies may be attributed to the application of

* Corresponding author.
E-mail address: magdalena.sandor@halliburton.com (M. Sandor).

http://dx.doi.org/10.1016/j.petrol.2016.09.004
0920-4105/

correlations that were originally developed for conventional oils (i.e., light oils), which are conceptually unsuitable for heavy oils (Cheng et al., 2009). Heavier hydrocarbons corresponding to the fast relaxation of T_1 and T_2 components should be included in the relaxation time-viscosity correlation. However, these signals are often non-detectable with NMR logging tools owing to hardware limitations, which render the NMR signal amplitude of the heavy-oil instrument and acquisition parameter dependent. Therefore, the restoration of signal amplitudes and rectification of relaxation-time distributions have become common practice in the methodologies adopted for NMR viscosity-correlation development.

In this work, we present three different methodologies that use NMR relaxation data to predict heavy-oil viscosity. The first method uses a modified power-law (Cheng et al., 2009) approach to predict viscosity as a function of temperature by implementing *TE* in the power-law coefficient. The second method uses the apparent hydrogen index to correct the apparent T_2 relaxation time to arrive at an intrinsic T_2 relaxation time. The third approach uses the sensitive relationship between T_1/T_2 and viscosity as a function of TE to predict heavy-oil viscosity at ambient temperatures. These relationships demonstrate a striking improvement in prediction ability over some previously published correlations. In addition, observations regarding fluid-sample conditions, such as sample storage time, presence of emulsion, and the resulting implications on NMR heavy-oil correlations are discussed.

2. Experimental section

2.1. Sample handling

A total of 56 heavy-oil samples were analyzed in this study. Heavy-oil samples were stored in dark glass vials and kept in a flammables storage cabinet under ambient conditions. Samples were homogenized at 50 °C for 30 min before being transferred to the NMR sample holder. Approximately 5 g of fluid sample was used for NMR measurements.

2.2. NMR measurements

NMR measurements were conducted using a 2.2-MHz Oxford Geospec 2 Rock Core Analyzer. NMR T_2 measurements, as a function of TE, on nine heavy-oil samples were carried out at ambient and elevated temperatures from 25 to 41 °C using a Temco coreholder. Temperatures were stabilized for two hours at each temperature prior to data acquisition. Background probe signals were corrected in the time domain at each *TE* and temperature point before inversion. T_1 and T_2 measurements on 11 heavy-oil samples were performed at ambient conditions to characterize the dependence of the T_1/T_2 ratio with viscosity as *TE* is varied. The number of samples was chosen to cover the widest spread in the T_1/T_2 ratio. Using 31 oil samples, the dependence of apparent hydrogen indices with respect to viscosity and TE was determined by integrating T_2 distributions to obtain the total signal intensity and then referenced to the NMR signal of a known volume of water. The relationship between T_2 relaxation and apparent hydrogen indices as a function of *TE* was also studied under ambient conditions. *TE* took on the following values for the experiments: 0.1, 0.4, 0.6, 0.9, and 1.2 ms.

2.3. Viscosity measurements and sample storage

Heavy-oil samples were divided into two subsets for more detailed analysis, since they were sampled during different periods of time. The first subset contained 13 heavy-oil samples from four different wells in the same reservoir field. Their viscosities were measured with four different viscometers to investigate the instrumental effect on heavy-oil viscosity measurements. Three of those samples were selected to study the changes induced in heavy oil by sample storage at ambient conditions up to 82 days. Their initial viscosity range is from 300 to 2000 cP at 32.2 °C. Owing to a limited supply of these three heavy oils, there was not enough fluid sample for NMR measurements.

The second subset of heavy oils contains 40 samples from the same field as the first subset of samples. All of the viscosity measurements from this subset were carried out using an Anton Paar parallel-plate rheometer (MCR501) in the temperature range of 20–40 °C at 0.5 °C/min. A low shear rate of 40 s^{-1} was applied to minimize the non-Newtonian effects of heavy oil. The suite of heavy oils examined is within the range of 10–17 API gravity. One milliliter (1 ml) of heavy-oil sample was used for each viscosity measurement. The effects of sample aging on viscosity and NMR T_2 relaxation were also examined for two heavy-oil samples when stored under ambient conditions for over 150 days.

2.4. Testing different viscosity measurement techniques

Four different types of commercially available viscosity measurement techniques were investigated. The following techniques were tested: glass capillary viscometer, oscillating piston viscometer, Anton Paar Stabinger viscometer (SVM) 3000, and Anton Paar parallel plate viscometer. The results are summarized in Table 1.

From Table 1, it can be observed that large inconsistencies from these four techniques can be as high as 42%. However, a comparison of viscosity results between the parallel-plate and rotational viscometers show a much closer agreement. Therefore, careful consideration of the available viscosity measurement techniques should take place to achieve the most accurate viscosity. Viscometer measurement discrepancies can be understood by considering the fact that a homogeneous shear stress is hardly achievable in glass-capillary and oscillating-piston viscometers. In addition, glass-capillary and oscillating-piston viscometer often operate at high shear rates, which can cause shear-thinning and a reduction in viscosity as observed in Table 1. In addition, compared to glass-capillary and oscillating-piston viscometers, parallel

Table 1
Viscosity results from four different types of viscometers.

Well name	Sample ID	Viscosity from glass-capillary viscometer[a], cP	Viscosity from oscillating-piston viscometer[a], cP	Viscosity from SVM 3000[a], cP	Viscosity from MCR501[b], cP
A	1	839	898	1,110	–
	2	796	899	1,070	–
B	3	1,626	1,692	1,865	1,834
	4	736	742	931	873
	5	299	323	349	
	6	–	–	840	
C	7	786	863	1,080	
	8	906	1,006	1,100	
	9	336	363	426	
	10	787	836	1,030	
D	11	238	272	–	
	12	238	261	314	284
	13	1,180	1,309	1,510	

[a] Measured in commercial service lab. The Anton Paar SVM-3000 measurement cell contains a tube filled with the sample, which rotates at a constant speed. The rotor used in the viscosity measurement floats in the tube.

[b] Parallel plate method was selected, as a minimal amount of sample is required for measurement.

Please cite this article as: Sandor, M., et al., Improved Correlations for Heavy-Oil Viscosity Prediction with NMR. J. Petrol. Sci. Eng. (2016), http://dx.doi.org/10.1016/j.petrol.2016.09.004

plate viscometers can operate under minimal stress.

Although not available for this study, a cone-and-plate viscometer would be highly effective for viscosity measurements since they have homogenous shear rates. While parallel plate viscometers do not have homogenous shear rates and are represented by an averaged shear rate, their shear rate is well-defined. The advantage they offer over cone-and-plate technique is that during temperature sweeps, thermal expansion will cause flexiable variations of the gap. Given the complex nature of heavy oil (i.e. self-aggregation into larger asphaletene molecules of unknown size or uncharacterized particulate matter in suspension) material may get lodged at the cone gap causing additional uncertainty in the acquired data. Consequently, a parallel-plate rotational viscometer was selected for heavy-oil viscosity in this study.

3. Results and discussions

3.1. Heavy-oil NMR T_1 and T_2 relaxation-time distributions

Fig. 1(a) displays the T_2 distributions as TE is varied (0.1, 0.4, 0.6, 0.9, and 1.2 ms) under ambient conditions for a 1000-cP heavy-oil sample. In heavy oils, T_1 and T_2 distributions are very broad and reflect the overlapping relaxation distributions of all the different molecular components within the fluid. Transverse T_2 relaxation describes the decay of coherence among nuclear spins in the x-y plane as a result of time-varying magnetic fields. Longitudinal T_1 relaxation describes the energy-exchange process of returning to thermal equilibrium along the z-axis of the static applied field. T_1 and T_2 relaxation in fluids are caused by dipole-dipole interactions that are mitigated by the rate of molecular motion. In heavy oils, intramolecular dipole-dipole interactions are the predominant source of NMR relaxation (Cowan, 1997; McConnell, 1987). The NMR results presented here are the geometric mean of relaxation times and are defined as:

$$T_{1,2GM}=\exp\left[\sum_{i=1}^{n} m_i \cdot Ln(T_{2i}) / \sum_{i=1}^{n} m_i\right], \quad (1)$$

where m_i represents the signal intensity corresponding to the ith component of the T_2 distribution. In Fig. 1(a), a systematic shift of the left fast-relaxing shoulder is observed as TE is increased owing to components of heavy oil that undergo relaxation faster than TE. This demonstrates the need to properly model the relationship between the relaxation deficit of T_{2GM} and TE. Fig. 1(b) shows an example of the temperature dependence of T_2 distributions of a heavy-oil sample at TE =0.6 ms. Here, it is observed that as the temperature is increased, the T_2 distribution shifts consistently towards longer relaxation times as a result of the increase of rotational diffusivity.

According to theory (Cowan, 1997; McConnell, 1987), T_1 and T_2 relaxation behaviors depend on the rotational correlation time, τ_c, and Larmor frequency, ω_o. For low-viscosity fluids or high-temperature conditions, where molecular motions are fast, the motional narrowing condition (or the fast-motion limit), $\tau_c\omega_o \ll 1$, applies, resulting in $T_1/T_2=1$. At low Larmor frequencies and when rotational correlation times of molecular motions are slow, the motional narrowing condition is not satisfied, giving rise to $T_1/T_2>1$, and is proportional to viscosity and described further in Section 3.4. Fig. 2 presents an example of a T_1 and T_2 distribution for a 14,000-cP heavy-oil sample under ambient conditions taken at a TE =0.6 ms. Here, it is observed that the T_1 distribution is offset towards longer relaxation times, resulting in a T_{1GM}/T_{2GM} =5.3.

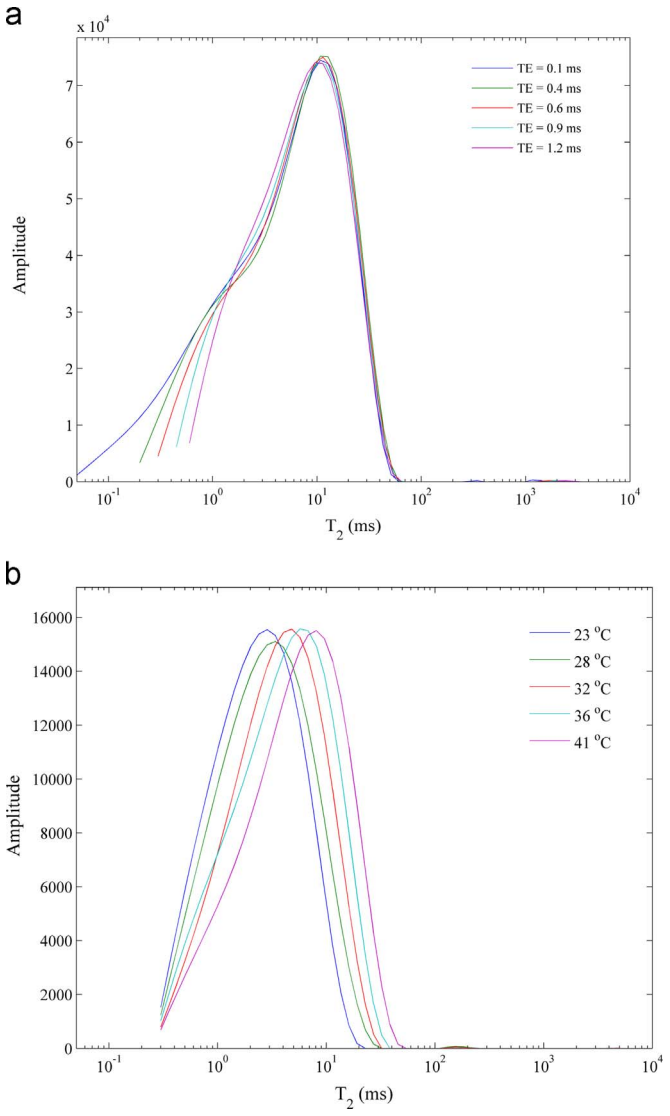

Fig. 1. (a) T_2 distribution data as a function of TE (0.1, 0.4, 0.6, 0.9, 1.2 ms). (b) T_2 distributions for oil samples, at TE =0.6 ms, as a function of temperature (21, 28, 32, 36, and 41 °C).

3.2. TE-modified power-law NMR viscosity correlation

Short-range dipole-dipole interactions are important for

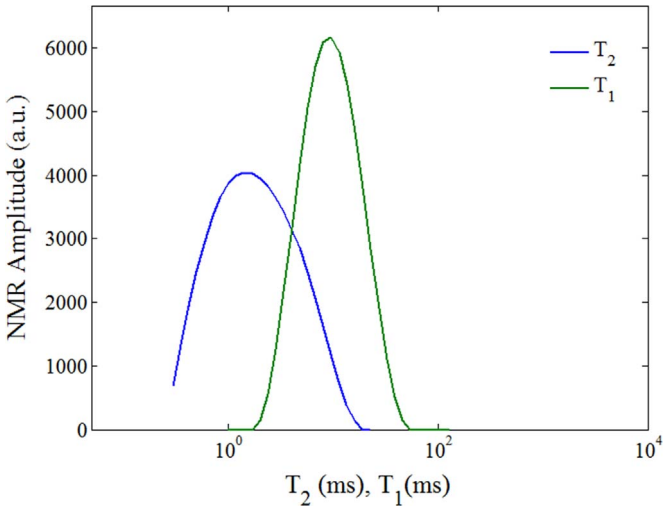

Fig. 2. T_1 and T_2 distributions for a 14,000-cP heavy oil acquired at a TE =0.6 ms.

describing the NMR response of reservoir fluids. For very light oils or high-temperature conditions, under the motional narrowing approximation, the T_2 NMR relaxation time is equal to its T_1 relaxation time, which is highly appropriate for very light oils or high-temperature conditions. The Stokes-Einstein and Debye relationships can be used to relate T_1 and T_2 relaxation rates to viscosity and thermal energy by (McConnell, 1987):

$$\frac{1}{T_1} = \frac{1}{T_2} \sim \frac{\eta}{kT}, \tag{2}$$

where, k is the Boltzmann constant, and T is the absolute temperature in Kelvin. Several of the existing NMR viscosity correlations are based on adaptations of this theoretical framework (Kleinberg and Vinegar, 1996; Bryan et al., 2005; LaTorraca et al., 1999; Zhang et al., 1998; Cheng et al., 2009; Ahmed et al., 2014; Zega et al., 1990). The relaxation behaviors of light oils can be adequately described by dipole-dipole time correlation functions that undergo exponential decay. However, heavy crudes contain structurally complex, high-molecular-weight components, such as asphaltenes and resins, where molecular motion is significantly hindered. Their dipole-dipole correlation functions can undergo non-exponential decay (Williams and Watts, 1970). A power-law functional dependence between NMR T_2 relaxation time and viscosity was recently published that considered a correlation function applicable to heavy oils (Cheng et al., 2009). This dependence is expressed as:

$$\frac{\eta}{T} \sim T_2^{\frac{-1}{\beta}}, \tag{3}$$

where, T is the absolute temperature and β $(0 \le \beta \le 1)$ is the stretching parameter. In the fast-motion limit, $\beta = 1$ for single or unique correlation times owing to random motion where Eq. (2) becomes important.

The relaxation behavior of heavier constituents of viscous oil is expected to exhibit the most sensitivity to changes in *TE*, resulting in a T_2 distribution deficit at longer echo spacings. Therefore, a correction factor that incorporates *TE* is typically used to convert from apparent to intrinsic T_2 relaxation, which may have a linear (Ahmed et al., 2014) or non-linear dependence (LaTorraca et al., 1999). Given the selective nature of *TE* on the relaxation distribution, the effect of *TE* on the power-law coefficient or stretching parameter, β, is also considered in the NMR viscosity correlation below. Fig. 3(a) is a plot of viscosity versus T_{2GM} for nine heavy-oil samples in the 21–41 °C temperature range while varying *TE* (0.1, 0.4, 0.6, 0.9, and 1.2 ms). The resulting correlation can be expressed as:

$$\eta = T_K \left(\frac{9.2}{T_{2GM} - 0.69TE - 0.86} \right)^{\frac{1}{-0.087TE + 0.90}}, \tag{4}$$

where T_K is the absolute temperature, η is the viscosity in cP, and *TE* is the echo spacing in milliseconds. The resulting correlation uses a linear relationship to correct both the apparent T_{2GM} and power-law coefficient owing to the relaxation time deficit. Fig. 3 (b) summarizes the comparison of the NMR-predicted viscosities to the rheological viscosities with a standard deviation of 0.22 on a logarithmic scale. For ease of comparison, red and magenta lines correspond to NMR predicted viscosities that are two and three times higher or lower, respectively. It is observed that most all of the predicted viscosities fall within a factor of 2, except at higher viscosities (~5000–10,000 cP) with an R^2 value of 0.88. It should be noted that the higher discrepancies of predicted viscosities obtained from $TE = 0.1$ ms may be attributed to minor probe signal contamination, which is most prominent at shorter TEs and may inadvertently decrease T_{2GM} and give rise to higher predicted viscosities. As a result of experimental uncertainties and conditions, some background signal may appear even after correction in the time domain.

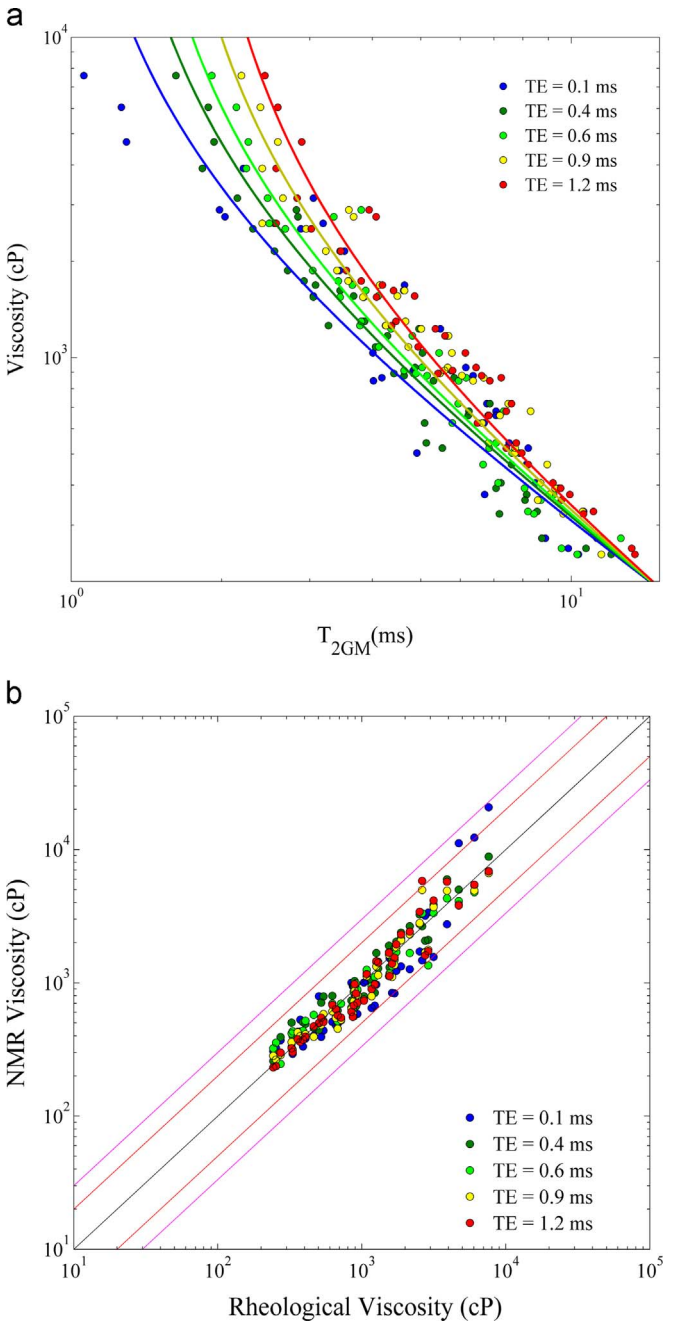

Fig. 3. (a) Fits to viscosity vs. T_{2GM} dataset and (b) comparison of NMR predicted viscosities and rheological viscosities. (For interpretation of the references to color in this figure, the reader is referred to the web version of this article.)

3.3. Viscosity predictions based on apparent hydrogen index-corrected T_{2GM}

Heavy oils consist of components, such as aromatics and asphaltenes that have considerably lower hydrogen content that may give rise to a reduced measure of HI (i.e. < 1). Owing to the constraints of NMR acquisition hardware, lower-measured HI values for heavy oils can also be expected as a result of heavy-oil constituents (Kleinberg and Vinegar, 1996; Bryan et al., 2005;

LaTorraca et al., 1999) relaxing at a rate faster than 1 ms. Interestingly, the limitations imposed by *TE* were found to play a far more significant role for measured values of HI than heavy-oil composition alone (LaTorraca et al., 1999). Given the NMR amplitude (or hydrogen index) and T_2 relaxation deficit based on NMR hardware restrictions, the apparent hydrogen index, at a given *TE*, can be used as a corrective factor to convert apparent T_{2GM} to a value closer to the intrinsic T_{2GM} for heavy oil. This comes from the systematic dependence of *TE* on the signal amplitude, as longer *TEs* are expected to result in higher HI losses.

Therefore, a correlation between the corrected NMR T_{2GM} and measured apparent HI of heavy oils with respect to *TE* can be developed to predict viscosity. This comes first from considering the calculation of T_{2GM} obtained from the inversion of measured magnetization decay. The HI is defined as:

$$HI = \frac{Amount\ of\ hydrogen\ in\ sample\ of\ a\ unit\ volume}{Amount\ of\ hydrogen\ in\ pure\ water\ of\ a\ unit\ volume\ at\ STP}. \quad (5)$$

The amplitude of the response of the NMR logging tool is calibrated with respect to that of bulk water at standard temperature and pressure (STP) conditions. For a general case, the HI of an oil sample in the reservoir can be expressed as:

$$HI = \frac{\sum_j^n \phi_j}{\phi(1-S_w - S_g)}, \quad (6)$$

where ϕ_j corresponds to the NMR intensity of the jth oil component, S_w is the water saturation, and S_g is the gas saturation. In Eq. (6), $\phi(1-S_w - S_g)$ is the true total intensity of heavy oil, which can be defined as ϕ_{HO}^{True}. The true total heavy oil intensity is a combination of the actual observed intensity, (ϕ_{HO}^{obs}), and the intensity loss, (ϕ_{HO}^{Loss}) due to T_2 relaxation components < echo time. Based upon Eqs. (1) and (6), the following relations exist:

$$\sum_{i=1}^{n} \phi_i \ln(T_{2i}) = \phi_{HO}^{True} \ln(T_{2GM}^{C}) \quad (6a)$$

$$\sum_{i=m+1}^{n} \phi_i \ln(T_{2i}) = \phi_{HO}^{obs} \ln(T_{2GM}) \quad (6b)$$

$$\sum_{i=1}^{m} \phi_i \ln(T_{2i}) = \phi_{HO}^{Loss} \ln(T_{2GM}^{Loss}) \quad (6c)$$

This can be used to give a HI-corrected T_{2GM} referred to as T_{2GM}^{C}:

$$\ln(T_{2GM}^{C}) = HI \ln(T_{2GM}) + (1-HI) \ln(f(0 \le t \le TE)), \quad (7)$$

where $f(0 \le t \le TE)$ is a function that relates the T_2 distribution at a time less than the echo time during NMR acquisition. Because it is assumed that the missing T_2 components have a lognormal distribution, f is set as 0.5TE. Theoretically speaking, hydrocarbon samples that have less than 20 wt% of asphaltenes should have a HI close to 1 and the samples in this study have less than 10 wt% of asphaltenes. However, for heavy oils, signals arising from heavy components are lost because of NMR hardware limitation. This gives rise to an apparent T_{2GM} that is higher than its intrinsic value. The role of the first term at the right-hand side of Eq. (7) is to reduce T_{2GM}, where it is over-weighted, and the role of the second term is to compensate for any lost T_{2GM} relaxation components. That is, HI provides a way to weight the NMR data. This results in an estimate of T_{2GM} that accounts for the shortcomings in the acquisition hardware.

Using Eq. (2), the NMR viscosity correlation can be expressed as:

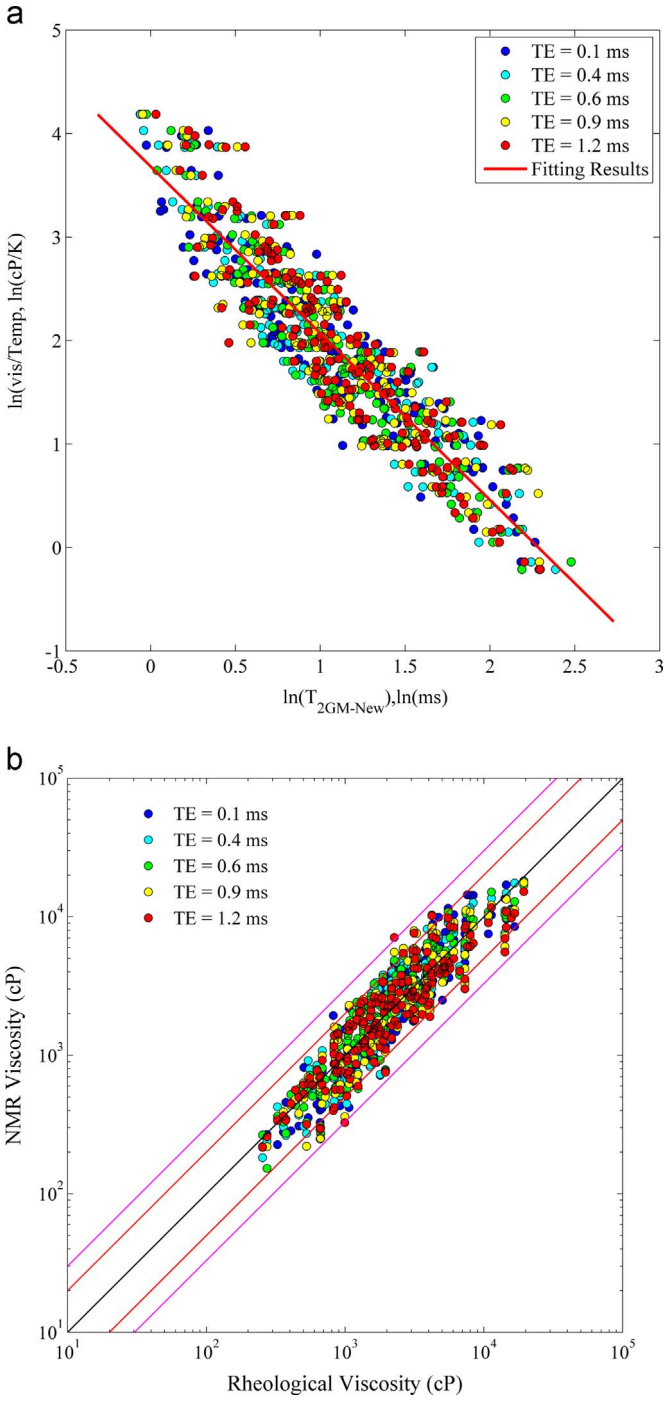

Fig. 4. (a) Power-law relationship between T_{2GM} and heavy-oil viscosity divided by absolute temperature. (b) Comparison between rheological viscosity and NMR-predicted viscosities, where red and magenta lines correspond to viscosities that fall within a factor of 2 and 3, respectively. (For interpretation of the references to color in this figure legend, the reader is referred to the web version of this article.)

$$\frac{\eta}{T} = b(T_{2GM}^{C})^{-a}, \quad (8)$$

where the fitting coefficients are $a = 0.53$ and $b = 8.18$. Fig. 4 (a) represents the fitting results when applied to 31 heavy-oil samples, where *TE* takes on values of 0.1, 0.4, 0.6, 0.9, and 1.2 ms and the temperature is varied between 21 and 41 °C. Fig. 4 (b) displays a reasonable comparison between NMR-predicted viscosities and rheological viscosities using Eq. (8) with $R^2 = 0.85$ and standard deviation of 0.34 on a logarithmic scale. Here, it is

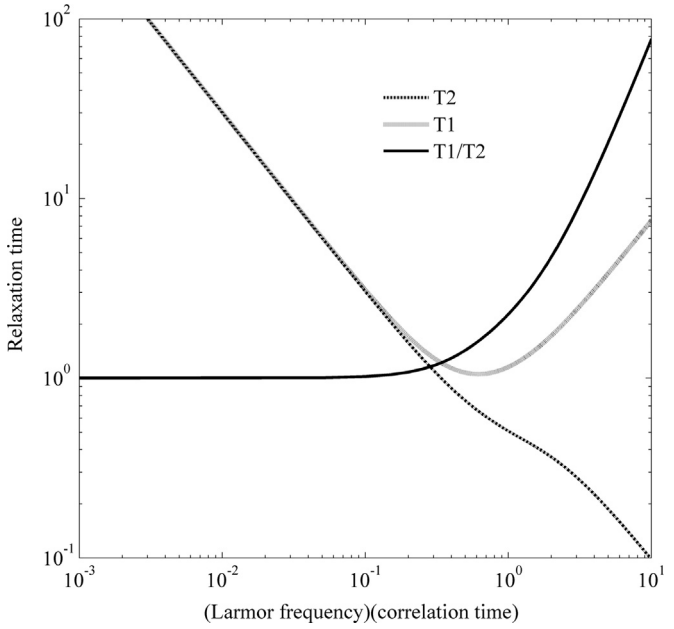

Fig. 5. T_1, T_2, and T_1/T_2 as a function of Larmor frequency multiplied by the correlation time.

observed that most predicted values are scattered uniformly within a factor of 2 of the measured viscosities. Large disparities are predominantly derived from NMR measurements acquired at longer TEs (> 0.1 ms). This may be partly attributed to the simplified function used for f.

3.4. T_1/T_2-based NMR viscosity correlation

For light crude oils or high-temperature conditions, motional narrowing conditions allow the ratio of T_1/T_2 to be ~ 1. As heavy-oil viscosity increases and motional narrowing is no longer satisfied, T_1/T_2 ratio increases (see Fig. 2). T_1 and T_2 relaxation rates governed by intra-molecular, dipole-dipole interactions are expressed as (Cowan, 1997):

$$\frac{1}{T_1} = \frac{9}{20}\left(\frac{\mu_o}{4\pi}\right)^2 \frac{\hbar^2\gamma^4}{r^6}\tau_c\left[\frac{\frac{2}{3}}{1+(\omega_o\tau_c)^2} + \frac{\frac{8}{3}}{1+(2\omega_o\tau_c)^2}\right]$$

$$\frac{1}{T_2} = \frac{9}{20}\left(\frac{\mu_o}{4\pi}\right)^2 \frac{\hbar^2\gamma^4}{r^6}\tau_c\left[1 + \frac{\frac{5}{3}}{1+(\omega_o\tau_c)^2} + \frac{\frac{2}{3}}{1+(2\omega_o\tau_c)^2}\right], \quad (9)$$

where τ_c is the correlation time, ω_o is the Larmor frequency, μ_o is the magnetic permeability, $\hbar$ is Plank's constant divided by 2π, and r is the distance to the nearest protons. Fig. 5 demonstrates the behavior of the T_1 relaxation time, T_2 relaxation time, and T_1/T_2 as a function of the correlation time and Larmor frequency. Here, it is observed that for short rotational correlation times or low viscosity, T_1/T_2 is independent of the viscosity. At higher viscosities, there is a non-linear relationship between T_1/T_2 and viscosity that exhibits more sensitivity to increases in correlation time than T_1 or T_2 relaxation alone. This demonstrates the value of using both T_1 and T_2 information to infer the viscosity of heavy crudes. Interestingly, this theoretical behavior is in conflict with what has been observed experimentally in heavy oils. For example, recent heavy oil studies (Yang and Hirasaki, 2008; Korb et al., 2015) have demonstrated that T_1 becomes independent above a threshold viscosity. However, compared to the suite of heavy oils in this study, which exhibit viscosities that are 1–3 orders of magnitude smaller, this anomalous behavior was not observed as demonstrated in the inset of Fig. 6(a) where T_1 relaxation time exhibits inversely proportional behavior with viscosity.

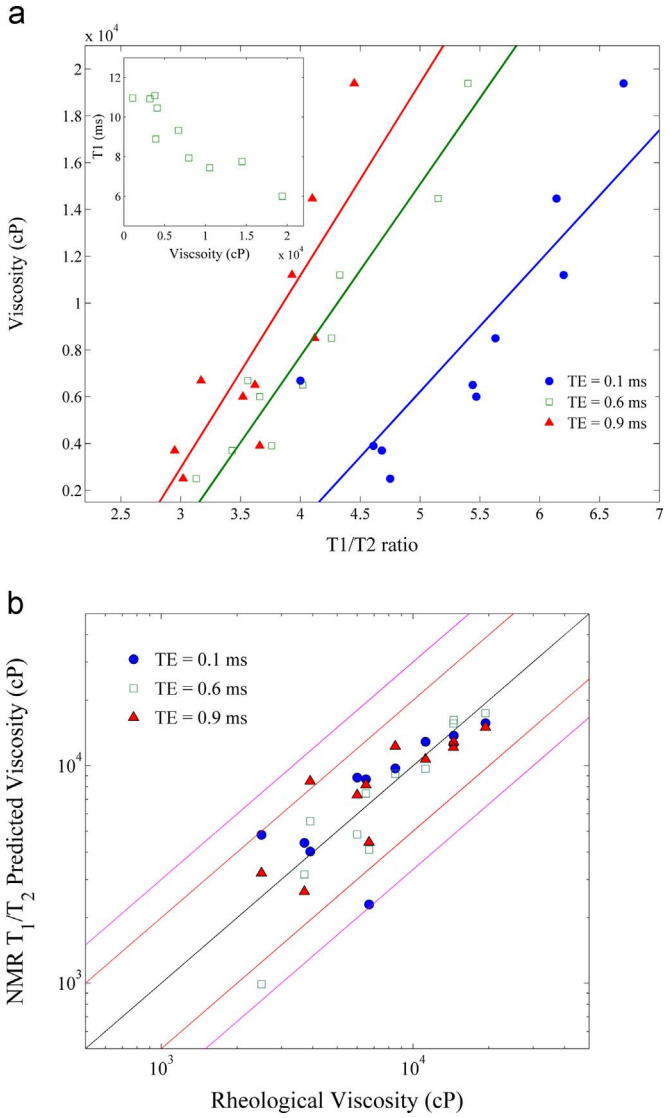

Fig. 6. (a) Viscosity as a function of the T_1/T_2 ratio for heavy oils at TE=0.1 ms (circles), 0.6 ms (squares), and 0.9 ms (triangles). The inset is a plot of T_1 relaxation time versus viscosity. (b) Comparison of rheological and NMR-predicted viscosities as a function of TE=0.1 ms (circles), 0.6 ms (squares), and 0.9 ms (triangles). (For interpretation of the references to color in this figure, the reader is referred to the web version of this article.)

Fig. 6(a) is a plot of viscosity vs. T_1/T_2 as a function TE at 0.1 ms (blue circles), 0.6 ms (squares), and 0.9 ms (red triangles) of eleven heavy crudes with an API gravity range of 10–14. These samples cover the T_1/T_2 range between 3 and 7. Because the T_1 and T_2 distributions of heavy oils are very broad (see Fig. 2), the geometric mean for each distribution was determined to compute the T_1/T_2 ratio. The systematic shift of the T_1/T_2 values of each heavy-oil sample with echo spacing is anticipated as longer dead times, resulting in a significant signal loss in signal at extremely short relaxation times. Therefore, in the range $3 \le T_1/T_2 \le 7$, the relationship between the viscosity and T_1/T_2 ratio can be expressed as:

$$\eta = (3340TE + 5250)T_1/T_2 - 21700, \quad (10)$$

where η is the rheological viscosity, T_1/T_2 is the ratio obtained from the geometric mean of the distributions, and TE is the echo

spacing. The constants in Eq. (10) correspond to the fitting coefficients obtained from the linear regression analysis. The data not only demonstrates the linear relationship between viscosity and T_1/T_2 ratio, but also the systematic changes with *TE*, which is important in the adaptation of the relationship to logging situations where there are constraints on the *TE* that is achievable. Given Eq. (9) and Fig. 5, the correlation is also expected to be proportional to Larmor frequency. The sensitivity of the relationship between the viscosity and T_1/T_2 ratio is suggested from the slope, which is proportional to TE, and becomes especially advantageous at longer TEs. However, it is important to note that linear behavior may not be satisfied at lower API gravities or from crude oils that are sampled from a different geological location owing to the high variability of molecular composition.

Fig. 6(b) shows a comparison of rheological viscosity versus the NMR predicted viscosities as a function of TE at 0.1 ms (circles), 0.6 ms (squares), and 0.9 ms (triangles). Here, it is clearly displayed that the correlation yields NMR-predicted viscosities that all fall within factors of 2 and 3, as indicated by the red and magenta lines, respectively, with an R^2 value of 0.80 and corresponding standard deviation of 0.30 on a logarithmic scale. Most of the scatter is observed at lower viscosities (<5000 cP), where the sensitivity of T_1/T_2 is more weakly dependent on changes in rotational correlation time (see Fig. 5).

The results of this work show that NMR relaxometry measurements correlate very well with heavy-oil viscosities and that each methodology has reasonable, yet similar success with heavy-oil predictions, as evidenced by the range of R^2 values (0.8–0.88).

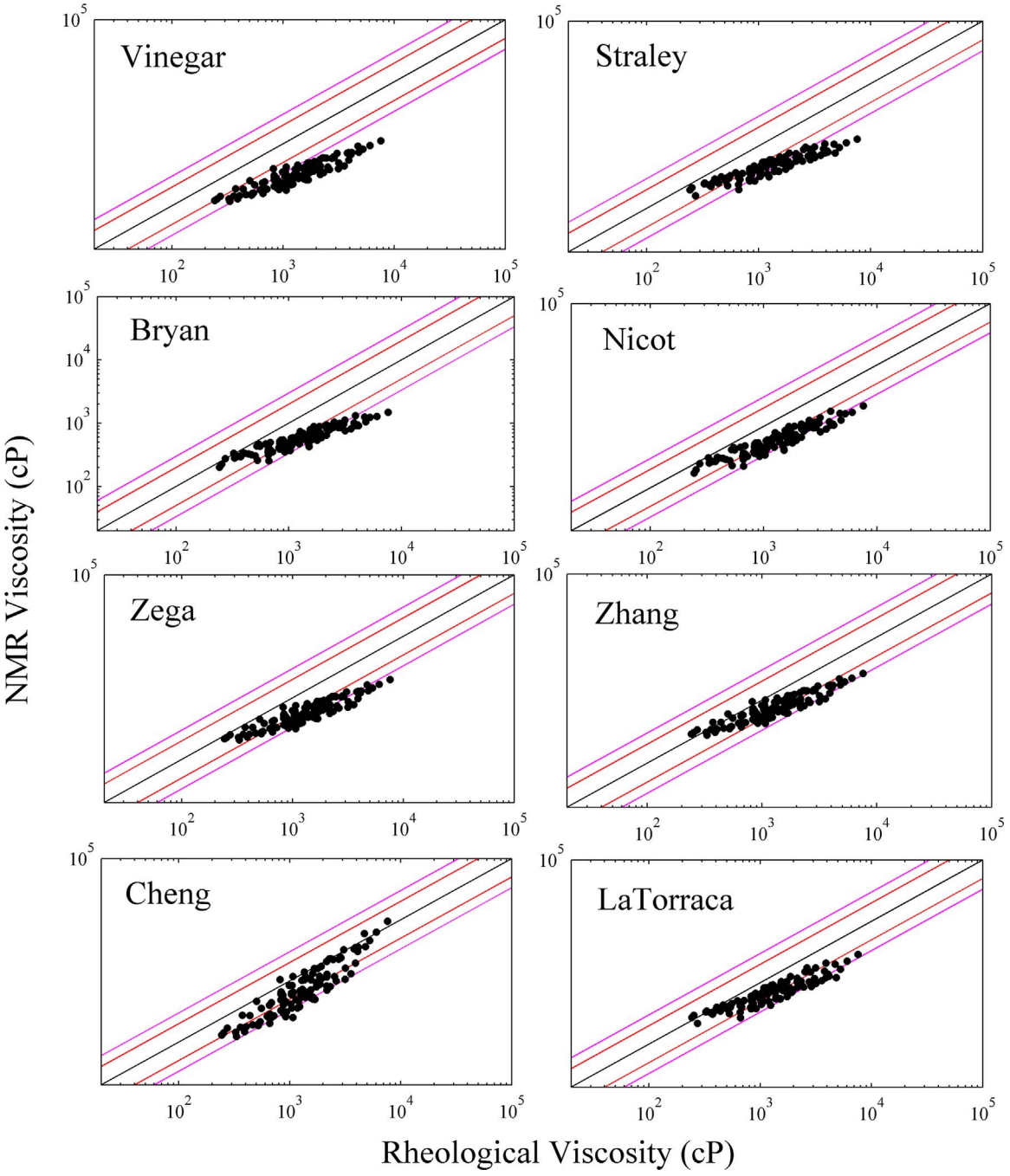

Fig. 7. Comparison of well-known semi-empirical viscosity correlations versus measured viscosities. Viscosity predictions by Cheng et al. (2009) demonstrate the most reliable predictions at higher viscosities >1000 cP. (For interpretation of the references to color in this figure, the reader is referred to the web version of this article.)

Please cite this article as: Sandor, M., et al., Improved Correlations for Heavy-Oil Viscosity Prediction with NMR. J. Petrol. Sci. Eng. (2016), http://dx.doi.org/10.1016/j.petrol.2016.09.004

However, it is important to emphasize that this also demonstrates the adaptability of implementing NMR in various scenarios given the availability of data. For example, given the situation where the apparent hydrogen index from neutron logging data and T_2 relaxometry data are available, one can use the correlation presented in Eq. (8). In the scenario, where specific NMR relaxometry data are available, either correlations implementing *TE* and T_2 (Eq. (4)) or the T_1/T_2 (Eq. (10)) correlation may be used with the anticipation of that both methods will yield similar viscosity predictions. Since less T_1 information is lost at longer *TEs* or for more viscous oil samples compared to T_2, it might be advantageous to consider correlation development exclusively for T_1 or to give priority consideration for correlations that implement T_1 data.

3.5. Tests of published heavy oil viscosity correlations

Fig. 7 summarizes plots of predicted viscosities versus measured viscosities of some well-known published correlations by Kleinberg and Vinegar (1996), Straley et al. (1994), Bryan et al. (2005), Nicot et al. (2006), Zega et al. (1990), Zhang et al. (1998), Cheng et al. (2009), and LaToracca et al. (1999). Red and magenta lines indicate agreement within a factor of 2 and 3, respectively. Heavy oil viscosities calculated using correlations by Zega, Nicot, Straley, and Bryan fall within a factor of 3 in the viscosity range 1000–3000 cP. The disparities between predicted and measured values continue to increase at viscosities >3000 cP. The power coefficient in Straley's correlation of 0.9 is comparable to that in Eq. (4) of 0.8–0.9 for the range of TE sampled in this work. However, the coefficient in Straley's correlation was tuned to predict the viscosities of crude oil between 0.7–1000 cP, which only covers a small fraction of the samples in this work. Bryan's correlation uses T_{2GM} and hydrogen index (*HI*) to predict viscosity. Laboratory measurements have demonstrated that the true hydrogen index is close to 1.0 for all samples, which may not serve as a sensitive enough variable for viscosity predictions as TE. This is also confirmed by similar experimental observations of hydrogen index in significantly heavier oils by LaTorraca (1999). Viscosity predictions using Kleinberg and Vinegar's correlation fall below the measured viscosities by over a factor of 3 in the entire viscosity range above 500 cP. It is observed that predictions by LaTorraca and Zhang fall within a factor of 3 across the entire viscosity range with some minor deviations near 3000 cP. The predicted viscosities using Cheng's correlation, which accounts for non-exponential decay behavior (i.e. glassy) in viscous oils, yields the best agreement at viscosities >1000 cP, where predicted viscosities fall close to the 1:1 solid line, despite the slight scatter at lower viscosities. This comparison of different correlations exhibits the successes and limitations, especially at higher viscosities, of implementing some of the current published viscosity correlations. At lower viscosities <1000 cP most all of the correlations perform similarly where predicted measured viscosities have lower disparities. This gives clear indication that the three correlations presented in this work show significant improvement in the predictive ability of heavy oil over the entire viscosity range compared to these published correlations.

3.6. Effects of heavy-oil sstorage time and emulsion on viscosity predictions

NMR core analysis of core and fluid samples is often used to calibrate the log response to a given rock and/or fluid property. Some limitations of this methodology come from conducting the analysis at reservoir conditions (i.e., temperature and pressure) and the alteration of the sampled fluid or core owing to sampling and the consequences of bringing the sample to the surface, such as significant fluid loss. This situation becomes increasingly complex for heavy-oil reservoir characterization, where high-viscosity variations have been attributed to reservoir heterogeneity, laboratory-based measurements (i.e., Table 1), and sampling techniques (Miller et al., 2006; Miller and Erno, 1995). The pursuit of high-quality samples has driven the industry to find and develop methods and techniques to stabilize and preserve the core and fluids at the wellsite so that in-situ reservoir conditions are preserved until the core- and fluid-analysis stage.

It is well established that water-in-oil emulsions are commonly formed during the production and sampling of heavy oil, since asphaltenes are natural emulsifiers or surface-active agents that aide in the formation of interfacial films around water droplets. Whether it is formed naturally in the reservoir is still under debate; however, a large body of evidence indicates the feasibility of creating emulsions in-situ (Cuthiell et al., 1995). Prior to the fluid analysis, heavy-oil samples are typically demulsified to remove any emulsion developed during sampling and transport. Preservation of composition and viscosity in heavy oils is a challenge owing to the susceptibility of evaporation (Fingas, 1997) of the lighter components of the crude oil. Heavy oils are expected to first lose compounds with the lowest boiling points and undergo a mass loss rate that varies logarithmically with time (Fingas, 1997). Evaporation may also be mitigated to some degree by complex interactions between heavy-oil compounds. Aerobic biodegradation of heavy oil, such as oxidation, may occur under ambient storage conditions, causing the oil viscosity to increase (Zhao and Machel, 2012). Simple precautions, such as storage of fluid samples under cooler conditions, can slow down or stop the evaporation process.

Fig. 8 shows the increase of heavy-oil viscosity at 32.2 °C of three different oil samples with starting viscosities of 300 cP, 1000 cP, and 2000 cP, respectively, when stored under ambient conditions for 82 days. The results demonstrate that the degree of heavy-oil aging owing to ambient storage is viscosity dependent. The lowest viscosity sample, oil sample 3, undergoes the highest viscosity increase of 21.3%, followed by oil sample 2 at 16.0% and lastly, oil sample 1 at $\sim$ 15.3%. Oil samples with lower viscosities have a relatively higher proportion of lighter hydrocarbons and are expected to be more sensitive to storage conditions.

The effects of sample storage are also reflected in the NMR

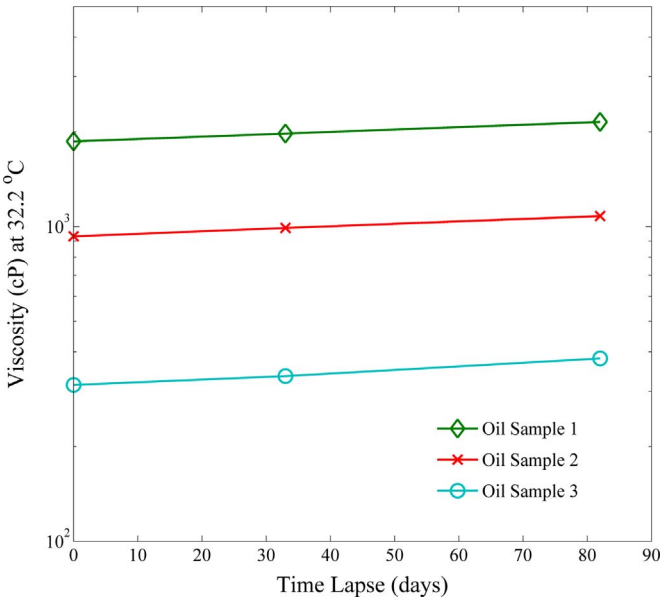

Fig. 8. Aging effect on three heavy-oil samples after storage under ambient conditions for 82 days.

Please cite this article as: Sandor, M., et al., Improved Correlations for Heavy-Oil Viscosity Prediction with NMR. J. Petrol. Sci. Eng. (2016), http://dx.doi.org/10.1016/j.petrol.2016.09.004

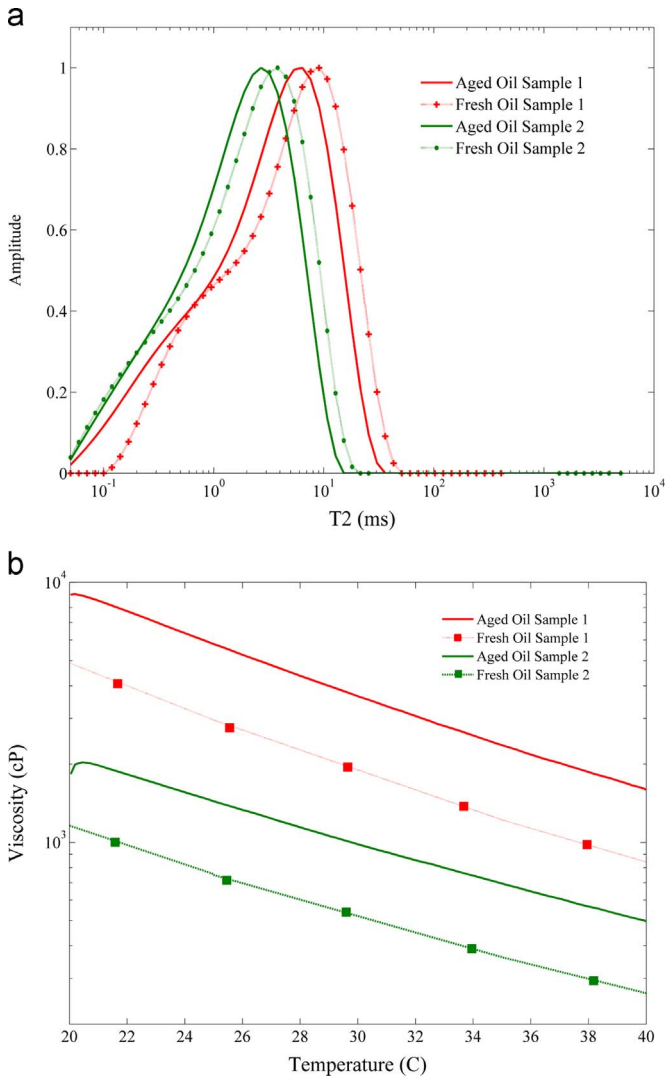

Fig. 9. (a) NMR T_2 distributions for two samples in fresh-condition (solid line) and five-month-storage-condition (dashed). (b) Viscosity measurements from 20 to 40 °C for fresh (solid line) and five-month-old samples.

characteristics of heavy oil. Fig. 9(a) shows the resulting T_2 distributions for two oil samples (dashed curves) soon after sampling and demulsification, as well as the result after subsequent storage under ambient conditions for five months (solid curves). Aging for five months results in a leftward shift of the distribution owing to the evaporation of the lighter oil components. Fig. 9 (b) summarizes the effects of aging on viscosity measurements in the 20–40 °C temperature range. For example, oil sample 1 in the fresh, demulsified state ranges from 5000-800 cP and then from 9000-1500 cP after significant evaporation.

The effect of heavy-oil aging on both NMR properties and viscosity raises an important question regarding fluid-sample conditions necessary for carrying out NMR viscosity correlation development. It is clear that ambient sample storage causes the aging of heavy oils and results in fluctuations of composition, NMR relaxation times, and viscosity properties that deviate from their native formation fluid properties. However, it is not clear how predicted and measured viscosities of aged oil samples would compare from a correlation developed from fresh, demulsified fluid samples. This is especially important considering the significant window of time between when a fluid is first sampled and when it is actually tested in the laboratory.

Fig. 10(a) redisplays Fig. 3(b) using Eq. (5) to compare measured

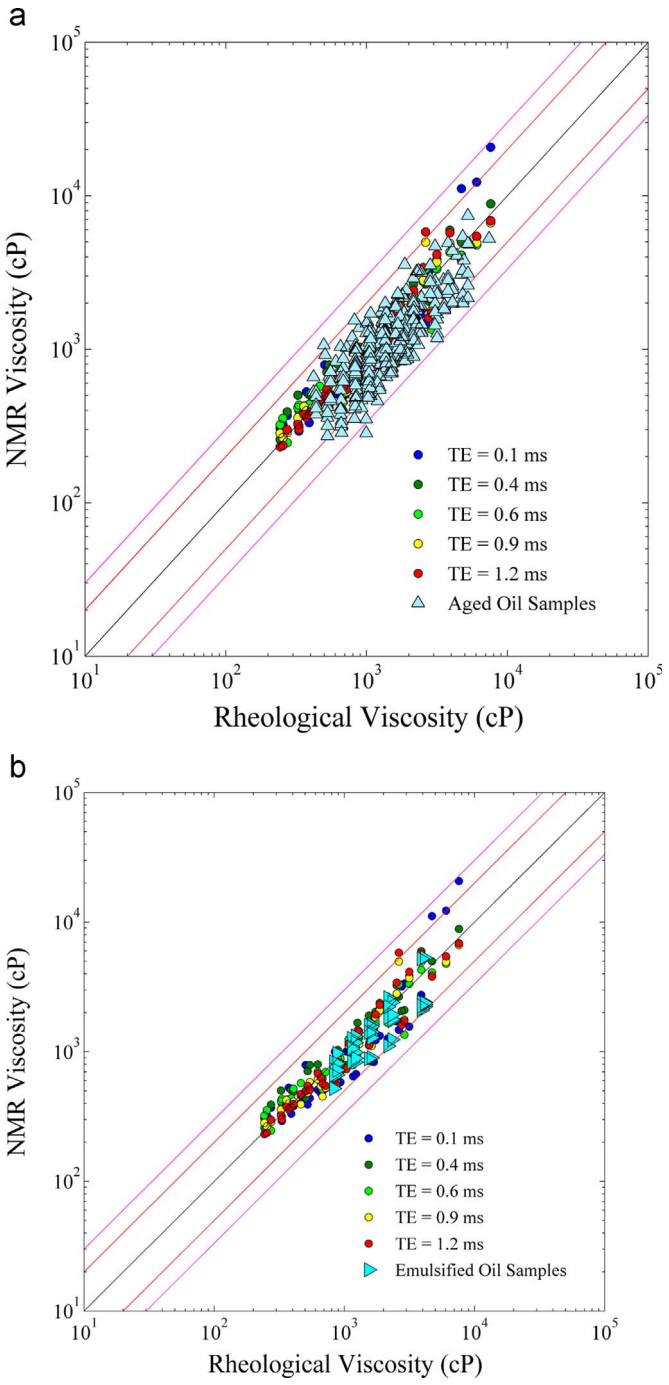

Fig. 10. (a) Comparison of NMR-predicted viscosities and rheological viscosities using aged heavy-oil samples. (b) Comparison of NMR-predicted viscosities and rheological viscosities using emulsified heavy-oil samples.

and predicted viscosities of aged oil samples stored under ambient conditions, ranging in time from 8 to 22 months. Here, aged samples have predicted viscosities that mostly fall within a factor of 2 or 3, where a significant portion of prediction points are scattered along the lower end (below solid line), giving a more optimistic prediction of heavy-oil viscosity. Predicted viscosities are, on average, approximately 34% lower than measured viscosities. Similarly, Fig. 10(b) shows the results from freshly sampled heavy-oil samples prior to demulsification, which show that predicted viscosities are, on average, approximately 24% lower than measured viscosities.

The discrepancy between measured and predicted viscosities of

Please cite this article as: Sandor, M., et al., Improved Correlations for Heavy-Oil Viscosity Prediction with NMR. J. Petrol. Sci. Eng. (2016), http://dx.doi.org/10.1016/j.petrol.2016.09.004

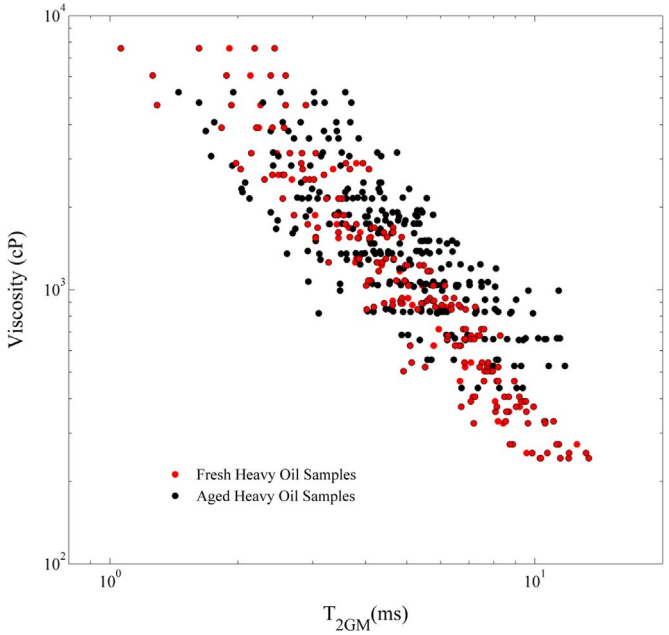

Fig. 11. Comparison of the viscosity vs. T_{2GM} between fresh and long-term stored heavy-oil samples.

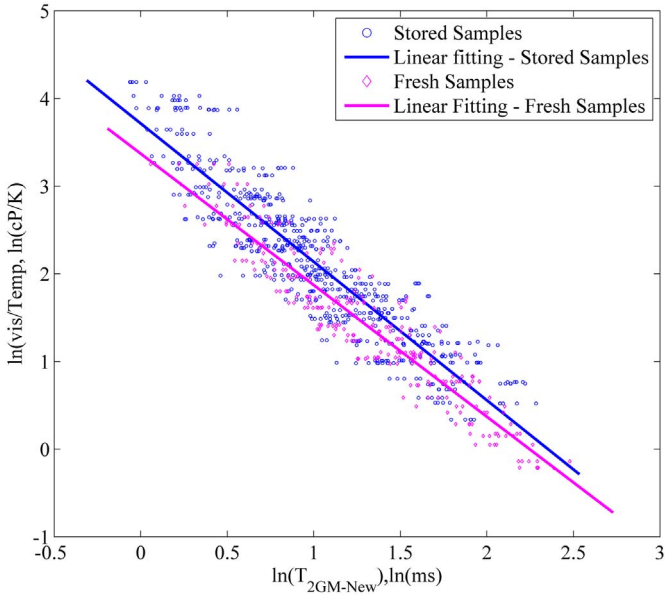

Fig. 12. Comparison of fittings between $ln\,(\eta/T)$ vs. $ln\,(T_{2GM})$ for fresh and stored heavy-oil samples.

aged heavy-oil samples can be understood from Fig. 11, which summarizes viscosities and T_{2GM} values from fresh and aged oil samples for all TEs (0.1, 0.4, 0.6, 0.9, and 1.2 ms) and temperatures (21–41 °C). Aged samples exhibit a much higher spread in T_{2GM} at a specified viscosity, with an average variance that is over two times higher than fresh heavy-oil samples. Lower NMR-predicted viscosities of aged oil samples can be attributed to the predominant spread of T_{2GM} values at longer relaxation times.

However, it is necessary to understand the implications of how a correlation derived from long-term stored samples would impact the viscosity prediction in the logging situation. This is also important, because often times, the sampling and storage conditions for fluid samples are either not well- documented or controlled. Fig. 12 is a plot of $ln\,(\eta/T)$ vs. $ln\,(T_{2GM})$ and demonstrates how the NMR correlation would change if one used long-term stored, emulsified samples versus fresh samples. The correlation derived from the aged samples does deviate from the correlation derived from the fresh samples. However, the standard deviation of the predicted viscosities of the freshly sampled oils from these two correlations is within 17%. This is considered tolerable from a logging stand point, especially when considering other factors, such as noise, which may introduce greater uncertainties. Moreover, one may apply a correction factor to account for the aging effect.

4. Conclusion

This study presents three different methodologies that use temperature and *TE*-dependent NMR T_1 and T_2 relaxation and HI data to predict heavy-oil viscosity. The first correlation considered a modified power-law relationship that implemented *TE* to correct for the effects caused by NMR non-exponential decay correlation time functions. The second methodology presented implemented HI as a means to offset any undercall or overcall of T_2 relaxation contribution. The third correlation uses both T_1/T_2 and *TE* to predict viscosity, where the sensitivity is enhanced at higher viscosities. These three correlations demonstrate the versatility and practical implementation of NMR relaxometry data to predict viscosity for a given data scenario. In addition, compared to several published correlations that implement similar NMR parameters, these relationships demonstrate a significant improvement in the predictive ability over the entire viscosity range. Lastly, the impacts of heavy-oil sample conditions are considered from the viewpoint of an input into the viscosity correlation. It shows that the fluid-sample condition (i.e., demulsification) and storage time are imperative for the most accurate viscosity-model development and predictions. The viscosities predicted with the correlation derived from the aged samples are 17% higher than those predicted with the correlation from the fresh samples; whereas, viscosities predicted for stored samples using a correlation derived from freshly sampled fluids are, on average, 34% lower. This effect can be accounted for by implementing a correction factor to interpret downhole logging data.

Acknowledgment

The authors thank Halliburton for permission to publish this work.

References

Ahmed, K., Sandor, M., Chen, S., et al., 2014. Viscosity Predictions of Viscous Oil from a Kuwait Field by Low-field NMR. Paper SPE 172896 presented at the SPE International Heavy Oil Conference and Exhibition, (Mangaf, Kuwait), 8–10 December.

Ahmed, K., Rampurawala, M.A., Nicot, B., et al., 2012. Practical downhole dielectric and diffusion-based NMR workflow for viscosity measurement in a viscous shaly sand reservoir using laboratory calibration: a case study from Kuwait. World Heavy Oil Congr.

Bryan, J., Kantzas, A., Bellehumeur, C., 2005. Oil Viscosity Predictions from Low Field NMR Measurements. SPEREE 8 (01), 44–52.

Cheng, Y., Kharrat, A.M., Badry, R., Kleinberg, R.L., 2009. Power-law Relationship between the Viscosity of Viscous Oils and NMR Relaxation. Paper SPWLA-2009-28327 presented at the SPWLA 50th Annual Logging Symposium. The Woodlands, Texas, 21–24 June.

Cowan, B., 1997. Nuclear Magnetic Resonance and Relaxation. Cambridge University Press, New York, NY.

Cuthiell, D., Green, K., Chow, R., Kissel, G., McCarthy, C., 1995. The in Situ Formation of Heavy Oil Emulsions. Paper SPE 30319 presented at the SPE International Heavy Oil Symposium. Calgary, Alberta, Canada, 19–21 June.

Fingas, M., 1997. Studies on the evaporation of crude oil and petroleum products: I.

the relationship between evaporation rate and time. J. Hazard. Mater. 56, 227–236.
Gawrys, K.L., Blankenship, G.A., Kilpatrick, P.K., 2006. Solvent entrainment in and flocculation of asphaltenic aggregates probed by small-angle neutron scattering. Langmuir 22, 4487–4497.
Kleinberg, R., Vinegar, H., 1996. NMR properties of reservoir fluids. Log. Anal., 37.
Korb, J.R., Nopparant, V., Nicot, B., Bryant, R.G., 2015. Relation and correlation between NMR relaxation times, diffusion coefficients, and viscosity of heavy crude oils. J. Phys. Chem. C 119 (43), 24439 -2446.
LaTorraca, G., Stonard, S., Webber, P., Carlson, R., and Dunn, K. 1999. Viscous Oil Viscosity Determination Using NMR Logs. Paper SPWLA-1999-PPP presented at the SPWLA 40th Annual Logging Symposium, Oslo, Norway, 30 May–3 June.
McConnell, J., 1987. The Theory of Nuclear Magnetic Relaxation in Liquids. Cambridge University Press, New York, NY.
Miller, K., Nelson, L., Almond, R., 2006. Should you trust your heavy oil measurement? JCPT 45 (4).
Miller, K., Erno, B., 1995. Use and misuse of heavy oil and bitumen viscosity data. CIM, 95-93.
Nicot, B., Fleury, M., Leblond, J., 2006. A New Methodology for Better Viscosity Prediction Using NMR Relaxation. Paper Z presented at SPWLA 47th Annual Logging Symposium. Veracruz, Mexico, 4–7 June.
Straley, C., Rosini, D., Vinegar, H., Tutunjian, P., Morris, C., 1994. Core analysis by low field NMR. Paper 9404 presented at Society of CORE Analysts.
Visintin, R.F.G., Lapasin, R., Vignati, E., D'Antona, P., Lockhart, T.P., 2005. Rheological behavior and structural interpretation of waxy crude oil gels. Langmuir 21, 6240–6249.
Williams, G., Watts, D.C., 1970. Non-symmetrical dielectric relaxation behavior arising from a simple empirical decay function. Trans. Faraday Soc. 66, 80–85.
Yang, Z., Hirasaki, G.J., 2008. NMR measurement of bitumen at different temperatures. J. Mag. Res. 192, 280–293.
Zega, J., House, W., Kobayashi, R., 1990. Ind. Eng. Chem. Res. 29, 909.
Zhang, Y., Lo, S., Huang, C., Hirasaki, G., Kobayashi, R., House, W., 1998, Some Exceptions to Default NMR Rock and Fluid Properties. Paper SPWLA-1998-FF presented at the SPWLA 39th Annual Logging Symposium, Keystone, Colorado, 26-28 May.
Zhao, Y., Machel, H.G., 2012. Viscosity and other rheological properties of bitumen form Upper Devonian Grosmont reservoir, Alberta, Canada. AAPG Bull. 96 (1), 133–153.

Please cite this article as: Sandor, M., et al., Improved Correlations for Heavy-Oil Viscosity Prediction with NMR. J. Petrol. Sci. Eng. (2016), http://dx.doi.org/10.1016/j.petrol.2016.09.004